Catalysis Letters Vol. 107, Nos. 1–2, February 2006 (© 2006)
DOI: 10.1007/s10562-005-9735-9

Characterization of new bimetallic oxycarbide ($MoWC_{0.5}O_{0.6}$) for bifunctional isomerization of *n*-heptane

A.-F. Lamic[a], C.-H. Shin[b], G. Djéga-Mariadassou[a], and C. Potvin[a,*]

[a]*Laboratoire de Réactivité de Surface, Université Pierre et Marie Curie, UMR CNRS 7609 Case 178, 4, place Jussieu, 75252 Paris cedex 05, France*
[b]*Department of Chemical Engineering, Chungbuk National University, Cheongju, Chungbuk, 361-763 Korea*

Received 8 November 2005; accepted 24 November 2005

A new bimetallic oxycarbide was synthesized and characterized by XRD, TEM, EDS, XPS and adsorption–desorption of probe molecules. All the molybdenum was reduced and 35% of tungsten was present as WO_x. The number of metallic sites, Lewis and Brönsted acid sites were estimated. A turnover rate of 0.1 s^{-1} was measured at 300 °C for the first order *n*-heptane isomerization.

KEY WORDS: bimetallic carbides; characterization; isomerization; TOR.

1. Introduction

Nowadays, hydroisomerization of paraffins is one of the largely used petrochemical processes. Transition metal carbides are well-known as noble metal substitutes [1,2] in olefins hydrogenation [3–5] or alkanes isomerization [6–8] reactions. The synthesis use of mixed molybdenum–tungsten carbides [9] is unusual and bimetallic carbides, niobium–tungsten carbides [10], molybdenum–nickel carbides [11], cobalt–molybdenum carbides [12] or cobalt–nickel–tungsten carbides [13] are rare. This study deals with the characterization of a new crystallographic bimetallic oxycarbide ($MoWC_{0.5}O_{0.6}$), subsequently tested in the bifunctional isomerization of *n*-heptane. In a previous paper, this reaction has been shown to be a bifunctional process [14]. The characterization of acid sites and determination of the number of Brönsted acid sites by adsorption–desorption of isopropylamine [9] allowed us to determine the turnover rate of the *n*-heptane isomerization.

2. Experimental

2.1. Materials

Molybdenum oxide (MoO_3, Aldrich, 99.99%), tungsten oxide (WO_3, Acros, 99.995%) were used as precursors. The gas employed were ethane, hydrogen, helium, argon (all supplied by Air Liquide, 99.5%). Isopropylamine (Fluka, 99.5 + %) and *n*-heptane (Aldrich, 99 + %) were used as received.

* To whom correspondence should be addressed.
E-mail: clp@ccr.jussieu.fr

2.2. Catalyst preparation

The oxycarbide ($MoWC_{0.5}O_{0.6}$) was prepared in two steps. First, the mixed oxide ($Mo_{0,47}W_{0,53}O_3$) has to be synthesized: MoO_3 and WO_3 (W/Mo molar ratio equal to 1) were crushed in a mortar; 1 g of the mixture was introduced under vacuum into a seal quartz vessel. The temperature was raised three times from RT to 750 °C at 100 °C h^{-1} and kept at this temperature for 6 h. The oxide $Mo_{0,47}W_{0,53}O_3$ was then introduced into a tubular quartz reactor and a 10 vol% C_2H_6 in H_2 (total flow rate = 10 L h^{-1}) mixture was flowed through the reactor. The temperature was raised from RT to 660 °C at 60 °C h^{-1} and kept at this temperature for 2 h. After rapid cooling to room temperature, the C_2H_6/H_2 flow was switched to an O_2/Ar mixture (1% v/v) for a passivation step.

2.3. Characterization

All samples were pretreated at 500 °C with flowing H_2 (1 L h^{-1}) for 3 h before elemental analysis and X-ray photoelectron spectroscopy (XPS) characterizations. They were then treated at 400 °C under vacuum for 1 h and finally sealed under vacuum in glass tubes. Elemental analysis were performed by the Service Central d'Analyses du Centre National de la Recherche Scientifique (Vernaison, France).

Specific surface areas were determined by the N_2 BET method on a Quantasorb Jr. apparatus. The samples were degassed under helium for 2 h at 300 °C.

A Siemens D500 automatic diffractometer with a monochromated Cu Kα source was used to determine the X-Ray Diffraction (XRD) patterns of the solid phases. Diffractograms were compared with the data of the Joint Committee on Power Diffraction Standards (JCPDS).

The selective chemisorption of CO was used to titrate the active metallic sites before catalytic runs and was performed by a pulse technique at 20 °C [5]. A known volume of CO controlled by an automatic valve passed through a reactor containing the sample (0.3 g), with He being used as the carrier gas. A thermal conductivity detector (TCD) detected the remaining non adsorbed CO at the outlet of the reactor. Hence, the consumption of CO was determined and the amount of CO chemisorbed by the sample deduced. Samples were first treated with flowing hydrogen in a reactor at 500 °C, and then quenched at 20 °C.

The number of Lewis and Brönsted acid sites was obtained by adsorption/desorption of isopropylamine before and after catalytic runs. The samples were pretreated under flowing He/H_2 (60/40 vol%) at 500 °C for 3 h. After determination of the total amount of acid sites (Lewis + Brönsted) at 100 °C by saturation of the catalyst by isopropylamine, a thermodesorption of amine was used to discriminate Brönsted acid sites (cracking of isopropylamine) from Lewis acid sites (no cracking of amine) [9]. The temperature was raised from 100 to 500 °C at 5 °C min^{-1}.

Transmission electron microscopy (TEM) studies were performed on a JEOL-JEM 100 CXII apparatus associated with a top-entry device and operating at 100 kV.

2.4. X-ray photoelectron spectroscopy

XPS measurements were performed on a VG Scientific ESCALAB 210 spectrometer with a Mg K_α X-ray source (1253.6 eV). The pressure in the analysis chamber was 5.10^{-10} Torr. The XPS spectra were recorded during sputtering with 3.0 keV Ar^+. All binding energies were referenced to C1s line at 284.6 eV from adventitious carbon. Their spectral decomposition was performed using WINSPEC (LISE-Université Notre Dame de la Paix, Namur, Belgium). Experimental peaks were decomposed to components (90% Gaussian, 10% Lorentzian) using a non-linear, least-squares fitting algorithm and a Shirley baseline. The W4f spectra typically consisted in an envelope which was decomposed to estimate the tungsten oxidation-state distribution. To reconstruct the levels of tungsten, some parameter constraints were imposed. A splitting energy of 2.15 eV and an intensity ratio I ($W4f_{5/2}$)/I ($W4f_{7/2}$) = 0.75 were used for the $W4f_{5/2}$–$W4f_{7/2}$ doublet. Both peak of the doublet were constrained to have the same full width at half the maximum (FWMH) peak height. To reconstruct molybdenum levels, the parameter constraints were the following: splitting energy of 3.2 eV and an intensity ratio I ($Mo3d_{5/2}$)/I ($Mo3d_{3/2}$) = 3/2 were used for the $Mo3d_{5/2}$-$Mo3d_{3/2}$ doublet. For the $Mo3p_{3/2}$–$Mo3p_{1/2}$ doublet, a splitting energy of 17.5 and an intensity ratio I ($Mo3p_{3/2}$)/I ($Mo3p_{1/2}$) = 2 were used. The relative ratios of W or Mo species were estimated on the basis of the integrated W4f or Mo3d band intensities by assuming that all W or Mo species have the same relative sensitivity factor.

2.5. Selective isomerization of n-heptane

The *n*-heptane reaction was carried out at 300 °C and atmospheric pressure to avoid any strong reduction of the catalyst and its partial pressure (6.7 kPa) was provided by a saturator kept at suitable temperature. The $H_2/n\text{-}C_7H_{16}$ molar ratio was fixed at 14.8. Passivated samples were pretreated under flowing H_2 (1 L h^{-1}) at 500 °C for 3 h. The composition of the effluent was analyzed using an online gas chromatograph system consisting of a 50-m HP-PONA capillary column coated with methylsiloxane. The total conversion reached steady state activity after 9 h on stream; the catalytic conversion and selectivity were measured at the steady state, the selectivity for the isomer products being defined as the percentage of *n*-heptane converted to *iso*heptanes.

3. Results and discussion

3.1. XRD and TEM studies

The mixed oxide phase corresponds to $Mo_{0,47}W_{0,53}O_3$ (JCPDS 32-1392). The carbide phase is characterized by large peaks (figure 1), which is in good agreement with the small particles observed by TEM (figure 2). The microdiffraction corresponds to a new cubic phase with a parameter intermediate between that of tungsten oxycarbide (JCPDS 22-959) and that of molybdenum oxycarbide (JCPDS 17-104). Using the five indexed peaks we obtained the cubic parameter $a = 4.217(8)$; this value was used for indexing the microdiffraction pattern (figure 2).

3.2. XPS analysis of $MoWC_{0.5}O_{0.6}$

The XPS technique was used to obtain information on the oxidation state of tungsten and molybdenum surface species. Two samples were studied. The first one was pretreated at 500 °C by flowing H_2 (1 L h^{-1}) for 3 h. It was then treated at 400 °C under vacuum, for

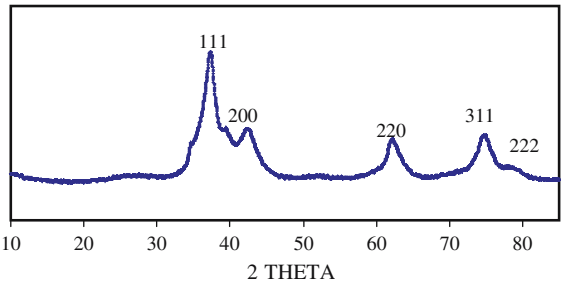

Figure 1. X-ray diffraction of $MoWC_{0.5}O_{0.6}$ catalyst.

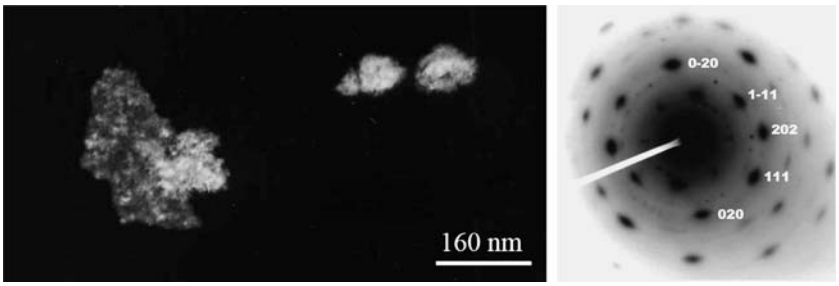

Figure 2. Transmission electron microscopy and the corresponding selected area electron microdiffraction of $MoWC_{0.5}O_{0.6}$ catalyst.

1 h, and finally sealed in a glass tube. The second sample was the stabilized catalyst, after 9 h under a *n*-heptane/H_2 stream. The XPS spectra for the W4f, Mo3d, O1s and C1s levels for the catalyst before catalytic reaction are presented in figure 3. The binding energies and the percentages of the different oxidation states of tungsten and molybdenum are summarized in table 1.

Three W species were detected after carburization. A typical decomposed XPS spectrum for the first material shows three W species, the highest binding energy (35.4 eV) being characteristic of W^{6+}, as in $Mo_{0.47}W_{0.53}O_3$ or WO_3. Two reduced forms were detected, a medium binding energy corresponding to $W^{\delta+}$ (32.7 eV) and at low energy W^0(31.7 eV). The amount of reduced tungsten is estimated at about 63%.

Two molybdenum species were detected. A species with a $Mo3d_{5/2}$ binding energy at about 229.5 eV was identified, midway between those assigned to Mo^{4+} (230 ± 0.2 eV) and Mo^{2+} (228.2 ± 0.2 eV) [15,16]; the species was assigned to $Mo^{\delta+}$. This binding energy has often been observed for molybdenum nitrides and carbides [17]. The species associated with a binding energy of 228.1 eV was assigned to Mo^0: all molybdenum is reduced. For the oxide $Mo_{0.47}W_{0.53}O_3$ the species with a Mo $3d_{5/2}$ binding energy of 232.4 eV was identified as Mo^{6+}. The percentages of the different oxidation states of molybdenum and tungsten after the induction period under nC7/H_2 flow are given in table 1. There is no significant difference, only a small reduction of the two metals being observed, indicating that the isomerization of *n*-heptane has a small influence on the oxidation states of this material.

3.3. BET surface area, titration of metallic sites, and Lewis and Brönsted acidity

Bifunctional isomerization of *n*-heptane involves catalysts containing a metallic function and an acidic one [18]. As the intermediate of the reaction is a carbocation, Brönsted acid sites are required. Table 2 gives the physical properties of the oxycarbide. The BET surface area is 54 m^2/g. CO chemisorption allows evaluating the number of hydrogenating sites. For acid sites, two samples were studied. The first one was obtained after H_2 pretreatment at 500 °C, and the second sample was the stabilized catalyst after 9 h under *n*-heptane/H_2 stream. Saturation of the surface by pulses of a known volume of isopropylamine gives the total uptake of amine, corresponding to the total uptake of attainable acid sites, assuming one adsorbed molecule of amine per site. The temperature programmed desorption (TPD) was used to identify and quantify the number of Lewis acid sites. When isopropylamine was detected in the outlet gas ($m/e = 59$ signal), the catharometer (TCD) permits to estimate the number of amine molecules adsorbed on Lewis acid sites. The Brönsted acid sites are calculated through the difference between the total acid sites and the number of Lewis acid sites. Figure 4 presents the TPD curve associated with the $m/e = 59$ signal (isopropylamine) detected with the mass spectrometer. This mass quantitatively represents an isopropylamine molecule which has not undergone any cracking, i.e. Lewis acid sites. All the desorption curves were considered as an envelop of peaks. The peak at 184 °C is clearly related to Lewis acid sites and the others at 266 and 290 °C to Brönsted acid sites. During the first 9 h of isomerization of *n*-heptane, the catalyst underwent a deactivation before reaching a steady state. All the desorption peaks are observed at a temperature near from that of the fresh catalysts. The total number of acid sites, and Brönsted and Lewis acid sites amounts are given in table 2. All type of acid sites decrease; for Lewis acid sites, it can be correlated to a low reduction of the two metals, as observed by XPS, and corresponding to a surface recarburization. As the initial catalytic activity is recovered after desorption of isopropylamine, we can attribute the loss of activity to some coke formed on Brönsted acid sites. The number of metallic sites and Brönsted acid sites are the same (6 μmol g^{-1}).

3.4. Isomerization of n-heptane

During the first 9 h of reaction, the catalyst underwent an induction period before it reached a pseudo-stationary state. As shown before, this induction period is due to the formation of coke on the Brönsted acid sites present on the surface. At the end of this time, the activity does not change and the contact time can be modified in order to determine kinetic parameters. Table 3 presents the main data for the catalyst, at a

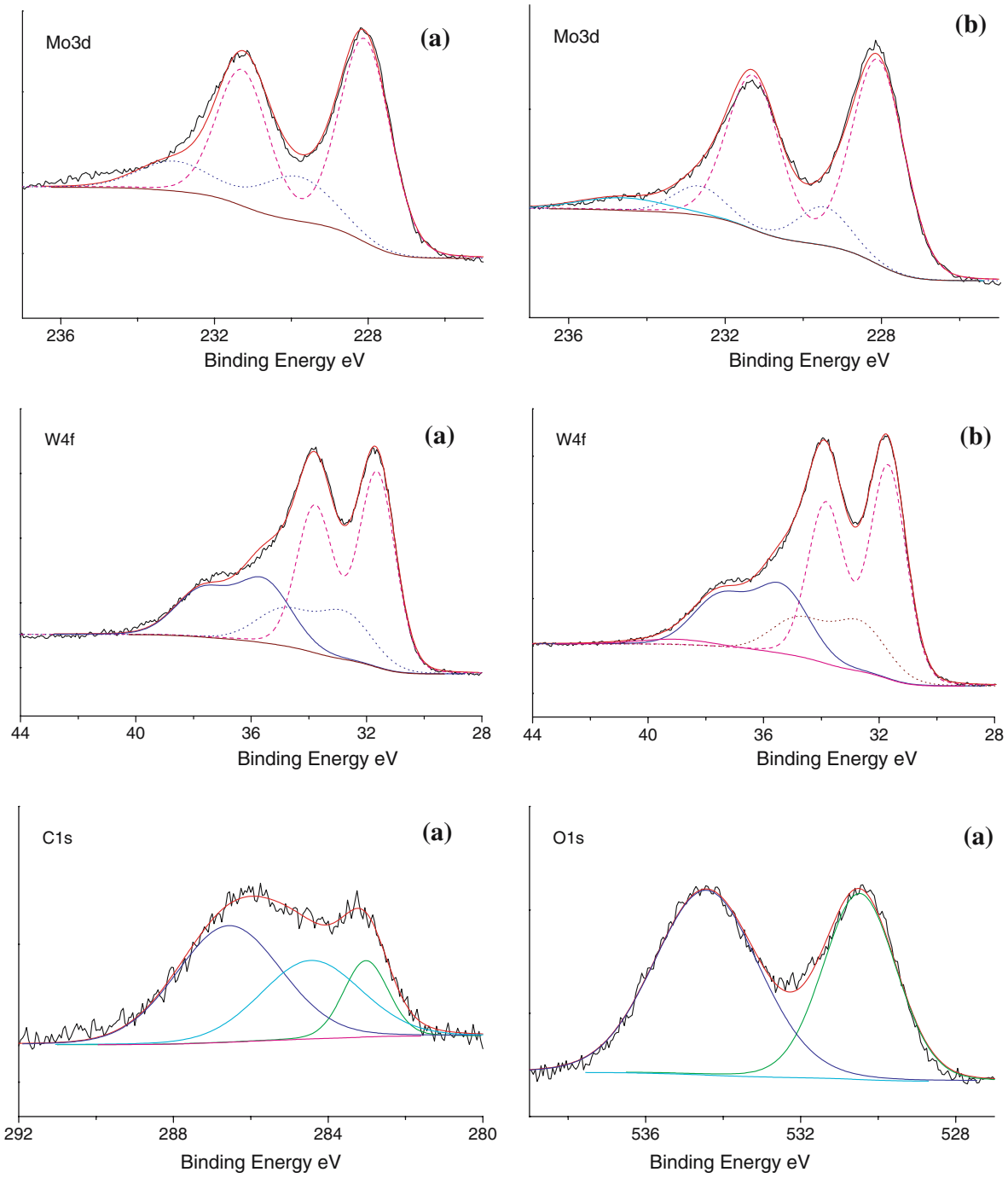

Figure 3. Overlap of the experimental XPS spectra, and the decomposition spectra for $MoWC_{0.5}O_{0.6}$ (after H_2 activation (a), after reaction (b)).

Table 1
X-ray photoelectron spectroscopy of $MoWC_{0.5}O_{0.6}$ (after H_2 activation and after *n*-heptane reaction)

	O1s		C1s		$Mo3d_{5/2}$			$W4f_{7/2}$	
	Oxide		Carbide		Mo^0	$Mo^{\delta+}$	W^0	$W^{\delta+}$	W^{6+}
After H_2	530.5	533.5	283.0	284.6	228.1	229.5	31.6	32.7	35.5
					82%	18%	63%	16%	21%
After reaction	530.5	533.5	283.2	284.6	228.1	229.5	31.7	32.7	35.4
					84%	16%	65%	15%	20%

Table 2
Number of metallic sites and acidic sites for $MoWC_{0.5}O_{0.6}$ (after H_2 activation and after induction period)

CO uptake (μmol g^{-1})	Total acid sites (μmol g^{-1})		Lewis acid sites (μmol g^{-1})		Brönsted acid sites (μmol g^{-1})	
	After H_2 activation	After induction period	After H_2 activation (T_{des}/°C)	After induction period (T_{des}/°C)	After H_2 activation (T_{des}/°C)	After induction period (T_{des}/°C)
6.0	9.4	7.0	1.8 (184)	0.7 (183)	7.6 (266; 290)	5.9 (262; 294)

conversion of about 20%. The selectivity towards isomers (defined as the percentage of *n*-heptane converted to *iso*-heptane) is around 95%. The major products (figure 5) were the two monomethylhexanes (SB); dimethylpentanes (MB) and short linear molecules (SM) produced by hydrogenolysis on the metallic sites; this reaction, taking place in parallel, represents 5% of the total *n*-heptane transformed, and it will be neglected in the kinetic analysis. These results are characteristic of successive reactions: *n*-heptane → SB → MB → cracking products [14,19]. Moreover, the $2mC_6/3mC_6$ molar ratio is closed to 1. Consequently, the mechanism of isomerization of *n*-heptane over these catalysts is bifunctional [19] as observed with oxygen modified W_2C [14] and Mo_2C [20] or on bimetallic carbides [9].

Figure 5 shows the conversion of *n*-heptane versus contact time and the corresponding linear transforms for a first order reaction. This catalyst follows the Sinfelt model [18]. It involves three catalytic cycles which are not kinetically coupled. The consequence of the model is that the metallic function has to be sufficient by strong to proceed, with no limitation, and that the acidic function has to proceed as fast as possible. The kinetics

Table 3
Product distribution for *n*-heptane isomerization on $MoWC_{0.5}O_{0.6}$ catalysts ($2mC_6$: 2methylhexane; $3mC_6$: 3methylhexane; iC_7: total of *iso*-heptene)

Contact time (s)	0.5
Conversion (%)	23.8
Select. into iC_7 (%)	94.8
Methylhexane (SB) (%)	81.8
$2mC_6/3mC_6$	0.99
Dimethylpentane (MB) (%)	7.9
n-heptene (mol.)	4.0×10^{-08}
Hydrogenolysis	5.2
Cracking	0

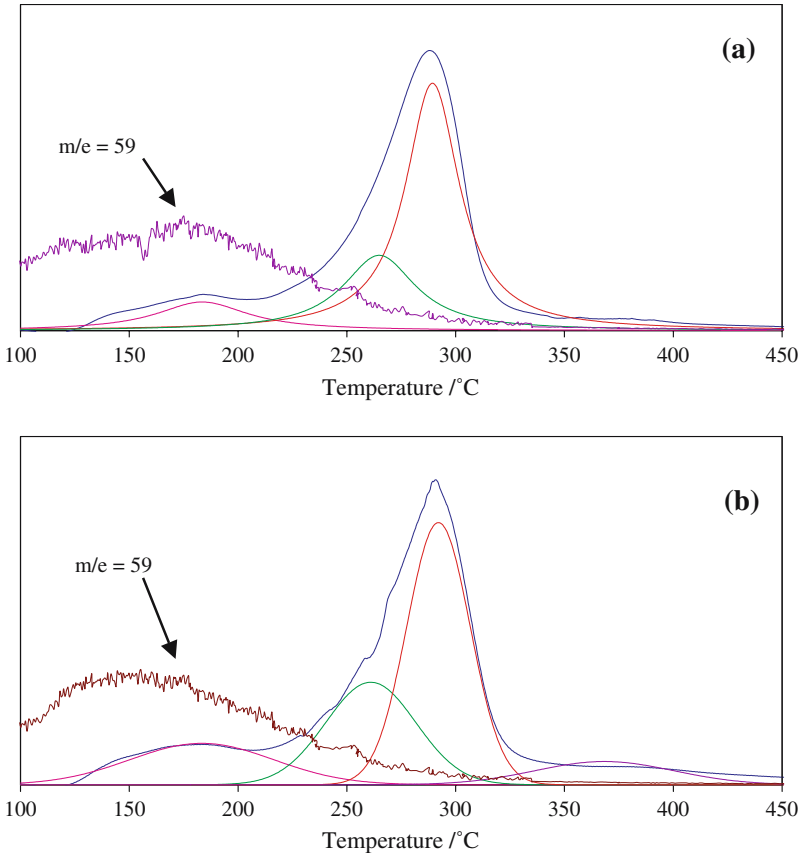

Figure 4. Temperature desorption profile of $MoWC_{0.5}O_{0.6}$ catalyst after H_2 activation (a) and *n*-heptane reaction (b).

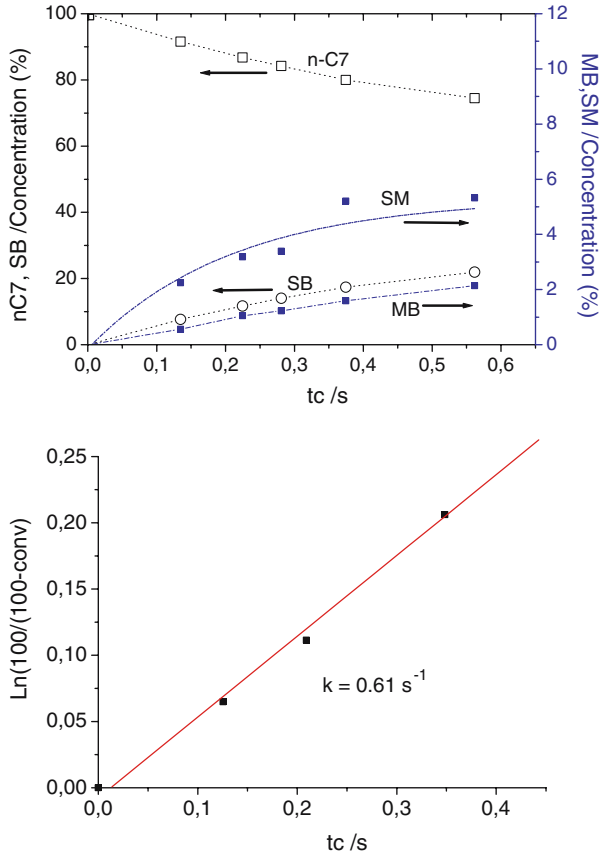

Figure 5. Concentration of *n*C7, single-branched (SB), multi-branched (MB) and short linear molecules (SM) versus contact time for $MoWC_{0.5}O_{0.6}$ catalyst. Linear transform of consumption of nC_7.

for this kind of catalyst has been previously discussed in another paper [14]. Moreover, the amount of heptenes is closed to that given by thermodynamics (4. 10^{-8} mol) indicating that cycle 1 is closed to thermodynamic equilibrium. The one order linear transform allows us to calculate the rate constant of disappearance of *n*-heptane (0.61 s^{-1} $g_{cat}{}^{-1}$). Knowing the number of Brönsted acid sites which are working, we can calculate the turn over rate (TOR) for the *n*-heptane transformation (0.1 s^{-1}). This value is the same that observed for the two phases Mo_2C-WO_2 catalysts [21] according to structure insensitive reaction.

4. Conclusion

A new crystallographically defined bimetallic oxycarbide ($MoWC_{0.5}O_{0.6}$) was prepared. It was shown to be able to isomerize *n*-heptane with a selectivity of 95% at 24% conversion at 300 °C, the major products obtained were the methylhexanes. This isomerization is a first order reaction and a bifunctional process. Molybdenum species are totally reduced and 35% of tungsten are present as oxide species responsible for the acidic function. The use of a new pulse technique to quantify the number of acid sites, by adsorption–desorption of isopropylamine, allowed us to determine the density of Brönsted acid sites. The numbers of both Brönsted acid sites and of metallic sites measured by CO chemisorption were the same (6 μmol/g). An induction period was observed, due to a loss of Brönsted acid sites and loss of Lewis acid sites (slight reduction). The turnover rate of isomerization of *n*-heptane over acid sites was determined at 300 °C: it is equal to 0.1 s^{-1}.

Acknowledgments

The help of Dr F. Warmont with the TEM and EDS measurements is greatly appreciated. We thank Dr L. Delannoy for constructive discussions and correcting the manuscript.

References

[1] R.B. Levy and M. Boudart, Science 181 (1973) 547.
[2] L. Volpe and M. Boudart, J. Sol. Stat. Chem 59 (1985) 348.
[3] I. Kojima, E. Miyazaki, Y. Inoue and I. Yasumori, J. Catal 73 (1982) 128.
[4] J.S. Lee, M.H. Yeom, K.Y. Park, I.-S. Nam, J.S. Chung, T.G. Kim and S.H. Moon, J. Catal. 128 (1991) 126.
[5] J.-S. Choi, G. Bugli and G. Djéga-Mariadassou, J. Catal. 193 (2000) 238.
[6] F.H. Ribeiro, R.A. Dalla Betta, M. Boudart, J. Baumgartner and E. Iglesia, J. Catal. 130 (1991) 498.
[7] E. Iglesia, J. Baumgartner, F.H. Ribeiro and M. Boudart, J. Catal 131 (1991) 523.
[8] P. Pérez-Romo, C. Potvin, J.-M. Manoli and G. Djéga-Mariadassou, Stud. Surf. Sci. Catal. 130 (2000) 2855.
[9] A.-F. Lamic, C.-H. Shin, G. Djéga-Mariadassou and C. Potvin Appl. Catal A submitted.
[10] V. Schwartz, V Teixeira da Silva and S.T. Oyama, J. Mol. Cat. A 163 (2000) 251.
[11] T. Xiao, H. Wang, A.P.E. York, V.C. Williams and M.L.H. Green, J. Catal. 211 (2002) 183.
[12] T. Xiao, A.P.E. York, H. Wang, H. Al-Megren, C.V. Williams and M.L.H. Green, J. Catal. 202 (2001) 100.
[13] S.L. Gonzalez-Cortes, T. Xiao, P.M.F.J. Costa, S.M.A. Rodulfo-Baechler and M.L.H. Green, J. Catal. 238 (2005) 127.
[14] A.-F. Lamic, T.-L.H. Pham, C. Potvin, J.-M. Manoli and G. Djega-Mariadassou, J. Mol. Cat. A 237 (2004) 109.
[15] R.B. Quincy, M. Houalla, A. Proctor and D.M. Hercules, J. Phys. Chem. 94 (1990) 1520.
[16] J.-C. Choi and L.T. Thompson, Appl. Surf. Sci. 93 (1996) 143.
[17] P. Pérez-Romo, C. Potvin, J.-M. Manoli, M.M. Chehimi and G. Djéga-Mariadassou, J. Catal. 208 (2002) 187.
[18] J.H. Sinfelt, H. Hurwitz and J.C. Rohrer, J. Phys. Chem. 64 (1960) 892.
[19] M. Guisnet, A. Alvarez, G. Giannetto and G. Perot, Catal. Today 1 (1987) 415.
[20] E.A. Belkkam, C. Pham-Huu, M.J. Ledoux and J. Guille, Ind. Eng. Chem. Res. 33 (1994) 1657.
[21] L. Leclercq, M. Provost, H. Pastor, J. Grimblot, A.M. Hardy, L. Gengembre and G. Leclercq, J. Catal. 117 (1989) 371.